Asian Journal of
Science, Technology, Engineering, and Art

e-ISSN: 3025-4507
p-ISSN: 3025-5287
Index: Harvard, Boston, Sydney University, Dimensions, Lens, Scilit, Semantic, Google, etc

https://doi.org/10.58578/AJSTEA.v3i2.5034

Feasibility Assessment of Wind Energy-Driven Automatic Irrigation System for Jos Plateau

Samson Daniel[1], Hassan Aliyu[2], Buhari Mamman[3], Yarima Sa'id Musa[4], D.M. Nazif[5]
[1,2,3,4]Abubakar Tafawa Balewa University Bauchi, Bauchi State, Nigeria
[5]Federal Polytechnic Bauchi, Bauchi State, Nigeria
tsakuma01@gmail.com

Article Info:

Submitted:	Revised:	Accepted:	Published:
Jan 25, 2025	Feb 9, 2025	Feb 21, 2025	Feb 26, 2025

Abstract

Nigeria's over-reliance on rainfall agriculture is reducing crop yield and keeping farm output below demand, despite irrigation farming providing insurance for rain-fed agriculture even during rainy seasons. The location of study is Jos, Plateau State, where year-round wind speeds of 3 to 9.37 m/s make providing electricity for irrigation water pumping feasible, and the nature of the terrain which enables the pump hydro storage technology. This study explores the feasibility of a wind-powered pump hydro storage scheme for smart irrigation systems, generating electricity to pump water and charge a battery bank. The farm uses a battery storage for irrigation control, powered by a microcontroller. The system monitors farm parameters using soil moisture and water level sensors. Raw wind data was upgraded from 10m to 50m hub height for improved power generation. The S3-1000-B8 wind turbine produces enough energy to pump a minimum of 8.7 m3 and a maximum of 176 m3 of water every week. Polynomial regression was used to calculate the wind power produced by this turbine, making it appropriate for this task. The 180 m3 of irrigation water needed per week to irrigate 10,000 m2 of agriculture was provided by 20 (S3-1000-B8) wind turbines. 720m3 of stored water is required for a month of safe irrigation. Based on wind potential, a single wind turbine can pump 234.864m3 of water and provide an average of 16kWh of energy every month. Consequently, the wind farm produces about 336 kWh and pumps 4,932 m^3 in total.

Keywords: Irrigation, Renewable Energy, Reservoir, Plateau

INTRODUCTION

Agriculture is crucial for sustainable development and poverty reduction in many third-world nations, and resolving this issue is essential for modernization and progress (Adenugba & Misra, 2019). The European Commission's Common Agricultural Policy (CAP) 2014-2020 proposes a greening program to enhance energy efficiency in agricultural production, utilizing innovative renewable energy technologies on farms.

Nigeria's agricultural industry comprises four sectors: crop production (87%), livestock (8.1%), fisheries (3.2%), and forestry (1.1%). Agriculture contributes 24% to GDP and employs over 36% of the labor force since 2013 (Oyaniran, 2020).

Plateau State, known for mining, primarily employs agriculture, primarily growing stable crops like acha, millet, yam, sorghum, corn, potatoes, cowpeas, rice, fruits, and vegetables. To meet agricultural demands, a smart irrigation system is crucial due to the region's unique geography.

Wind energy is a rapidly growing industry globally, primarily used for electricity and water pumping, driven by environmental concerns, rising fossil fuel costs, and economic development.(Azad et al., 2015; Mentis et al., 2015). Wind power is gaining popularity as a renewable energy source for electricity production and water pumping due to its environmental friendliness and ability to meet irrigation needs (Ohunakin & Akinnawonu, 2012).

The plateau state, situated on a wind speed potential of 3-8.6 m/s (NIMET), generates electricity for irrigation and utilizes water reservoirs from mining dams. This irrigated land area protects rain-fed agriculture from unpredictable rainfall and climate change impacts, ensuring resilience (Olayide et al., 2016).

Jos, the capital of Plateau state, is a suitable location because it is naturally windy and has an average wind speed above 5 m/s throughout the year. Jos's NIMET meteorological station's coordinates are latitude 09-52 N, longitude 08.45 E, and altitude 1217 m, and these measurements were made at a height of 10 m using a cup-generator anemometer (Ohunakin & Akinnawonu, 2012).

A typical wind turbine is depicted in Figure 1. The most popular types of wind turbines in use today are horizontal axis wind turbines (HAWTs). HAWTs, with upwind or downwind-positioned rotors and aerodynamic blades, typically have two or three blades, allowing them to move quickly at the blade tips.

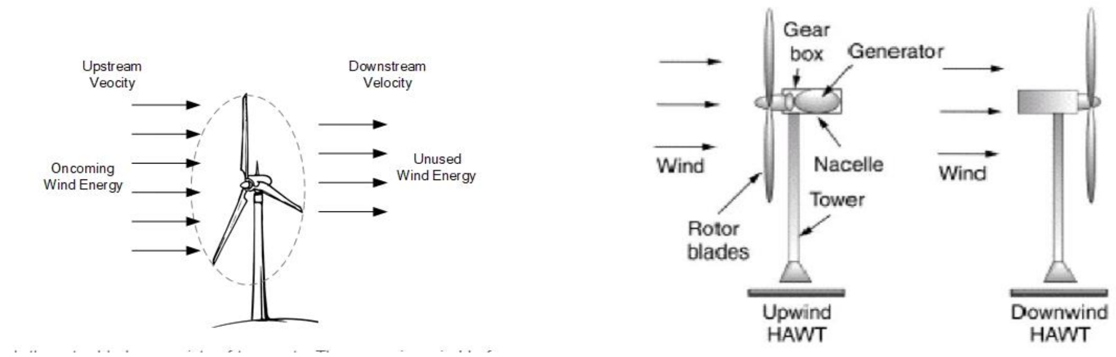

Figure 1: The horizontal axis wind turbine. (Francisco, 2019).

Downwind rotors have coned blades for self-orientation, while upwind rotors require a tail vane. However, their low-speed energy production is reduced due to their tendency to wander (Hyams, 2012).

The HAWT has excellent efficiency, power output, and operational wind speed reliability. The horizontal axis wind turbine was selected based on its efficiency because currently, it can convert 50% of the wind power received into electricity. Also, it should be possible to generate power with the least amount of wind possible to provide effective irrigation water.

The research uses pump hydro energy storage (PHES) where water is pumped from a lower reservoir to an upper reservoir, released for irrigation, and continued until full.

Literature Review

Usman et al., (2024) drew attention to the ongoing problem of small-scale farmers' lack of access to electricity, which hurts crop productivity, particularly during dry seasons. The study examines the performance of a small-scale wind energy conversion device for agricultural use, utilizing NIMET wind speed data to analyze electrical parameters, assessing fluctuations and ensuring system suitability for simulation (Saras et al., 2018). Akour et al., (2018) used the operational Reynolds number to optimize the blade geometry for an average wind speed of 5 m/s along with the blade element momentum theory. The economic feasibility study was conducted using a 3D-printed prototype blade. It is concluded by the findings that the ATT (Akour Team Turbine) is efficient and economically feasible to produce energy in low wind speed regions.

The study also discusses the possible advantages of lowering the use of diesel generators, which might result in cheaper generation costs and fewer emissions of greenhouse gases (Javed et al., 2019). This research examines hybrid solar-wind power supply systems using pumped hydro storage, highlighting their function, installed capacity, and technological challenges, emphasizing their role in renewable energy infrastructure (Duker et al., 2020). The study explores the feasibility of wind power for irrigation in the Cauvery Delta, emphasizing the need for a pre-feasibility study to assess its techno-economic viability.

MATERIALS AND METHODS

Wind data acquisition

The Nigeria Meteorological Agency provided wind data from August 2018 to December 2021. The data was used to determine the average power generation in Jos, plateau state for sustainable smart irrigation farming.

The prospect of wind power at the site (Jos)

From the data available for the site (Jos), the wind speed available and viable for the chosen turbine ranges between 1.3ms^{-1} to 9.37 ms^{-1}. Power from the wind can be estimated by Equation 1;

$$P_{(v)} = \frac{1}{2}\rho A V_m^3 \qquad (W) \qquad \text{...1}$$

The air density at the site is found to $\boldsymbol{\rho = 1.21 kg/m^3}$(Ohunakin & Akinnawonu, 2012). This will be used to calculate the energy in the wind and compare it with the turbine energy generated using the same wind speed.

Reservoir

The reservoir system will serve as the water storage unit to replace the battery backup unit because of the high cost of replacement and maintenance over a long period.

The reservoir is of two types, the lower-level reservoir, and the upper-level reservoir. The upper reservoir will hold water at a quantity required to cover the water needed during the autonomy period of at least 3 hours daily for 3 days a week for a month. The lower reservoir will hold water more than the upper reservoir which is expected to be replenished every year during the rainy season.

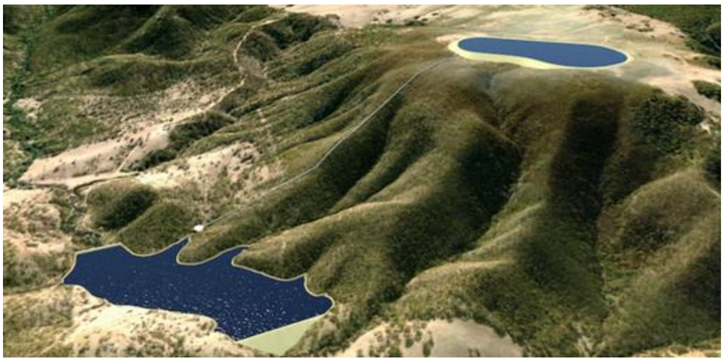

Figure 2: A lower and upper reservoir of a pump hydro storage (https://www.atco.com/en-au/about-us/stories/atco-pumped-hydro-storage-nsw.html)

Pump

The pumps are powered by wind turbines. Motorized pumps usually operate on 150V to 450V DC to drive a 220V AC water pump or 250V DC to 800V DC to drive a phase 380V AC water pump with the help of a variable frequency drive. Or DC pumps powered by 12V, 24V, or 48V supply. These pumps are responsible for pumping water to the upper reservoir for storage.

3.3 Irrigation Control System

The control system is responsible for the farm irrigation and monitoring of farm parameters. Below is the diagram of the control circuit that monitors and controls the irrigation of the farm and the pumping of water to the upper reservoir.

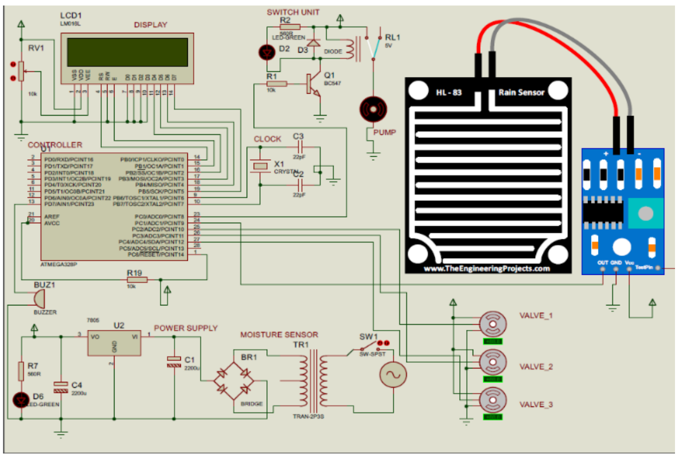

Figure 3: The Control Circuit

The microcontroller (Arduino UNO)

A crucial component of this irrigation system is a microcontroller. The output of all the sensors had been provided as the analog inputs to the Arduino. Analog inputs are converted to digital outputs by this microcontroller. There is a relay attached to these digital output signals. The program that is already burned into the microcontroller is what generates these digital outputs.

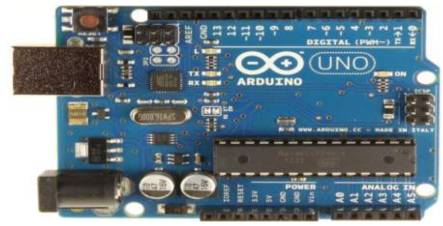

Figure 4: Arduino UNO

Connection of Soil Moisture Sensor to Microcontroller

The soil moisture sensor is connected to the Arduino using a digital PCB drive. The PCB drive has a digital potentiometer. The digital pot is used to modify the sensor's sensitivity when it is linked in digital mode. The PCB drive out has four connecting pins, according to the chart below.

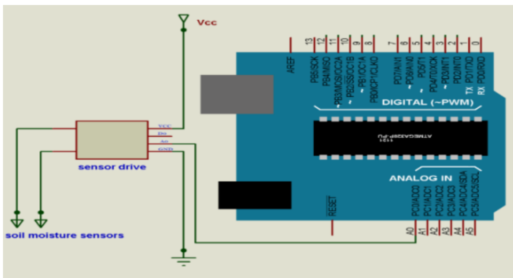

Figure 5: Connection to Arduino board

The sensor's output is a resistance base, which was connected to Arduino analog pin A0. The soil type and moisture content affect the impedance to the current passage between the sensor probes. The current (Iout) passing through the sensor probes for various soil types and soil moisture levels is calculated as follows:

$$Iout = \frac{Vcc}{\{Soil\ Resistance\ value\ (R_S)\}} \quad ...2$$

The moisture content of the soil is detected by a soil moisture sensor. The resistance determines how this moisture level sensor responds. Low resistance values indicate that the soil has a high moisture content. High resistance indicates that the soil is dry. This signal is given to the Microcontroller and this makes the relay to be operated.

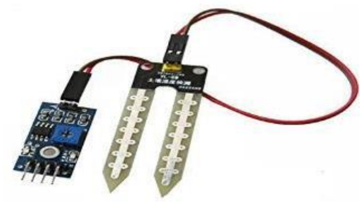

Figure 6: Soil Moisture Sensor

Additionally, it determines the volumetric water content of the soil by substituting another soil characteristic, such as electrical resistance, the dielectric constant, or neutron interaction, for the moisture content. It is necessary to calibrate the relationship between the measured property and soil moisture since it can change based on the environment, including the soil type, temperature, and electric conductivity.

Water level detector

To gauge the water level, a water level sensor is inserted into the tank or reservoir.

The sensor is provided with the reference value as the minimum necessary level. The user is provided with information about the water level if the water level drops below the reference level.

Figure 7: Water Level Sensor

The Irrigation Control System block diagram.

An Arduino Uno is used in this project to control the motor and valve. The schematic is used to connect the Arduino to the motor driver and the driver to the water pump. The motor can be powered by 12, 24, or 48 volts.

The moisture sensor determines how moist the soil is and alerts the Arduino if more watering is required. Up until the necessary moisture level is reached, the plants are given water by gravity.

The gravity tank/reservoir water level sensor aids the microcontroller in keeping track of the reservoir's water level. The water flow valve aids the microcontroller in directing water either to the reservoir for storage or to the farm for irrigation.

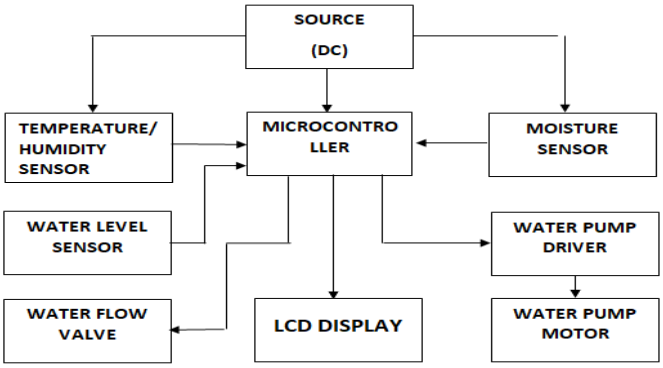

Figure 8: Block diagram of the control unit.

The flowchart.

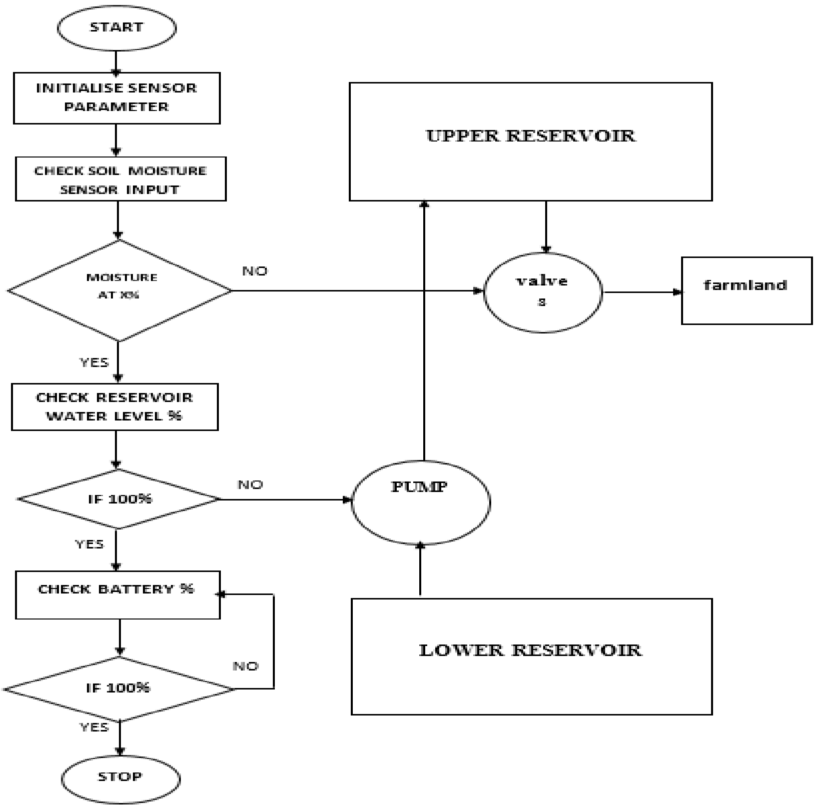

Figure 9: System Flowchart

RESULTS AND DISCUSSION

The results obtained from this research work are presented in this chapter. The wind data collected from Nigeria Meteorological Agency (NIMET) Jos, is analyzed and upgraded to a hub height for viable power generation and the result of the equivalent power calculated from the upgraded wind speed is presented. The energy and water storage are presented and the result from the Matlab simulation of the wind data is also presented.

The wind speeds are adjusted to the wind turbine hub height using the power law formulation. (Ohunakin et al., 2011),(Ohunakin, 2011),(Ohunakin & Akinnawonu, 2012) of equation 3.

$$\frac{u}{u_0} = \left(\frac{H}{H_o}\right)^{\alpha} \qquad ...3$$

Where H_o is the reference hub height, u_o is the reference wind speed, H is the new hub height and u is the new wind speed.

Figure 10 shows the chart of the average wind speed upgrade at 10m and 50m height for the first year (August 2018 to July 2019). The blue curve at the bottom is the average monthly wind speed at 10 meters in height, after upgrading the wind speed for every 10 meters, it is obvious the increase in speeds in August 2018 and February 2019 are the highest for the year. There is also some viable wind speed in July and between October to February for possible generation of power.

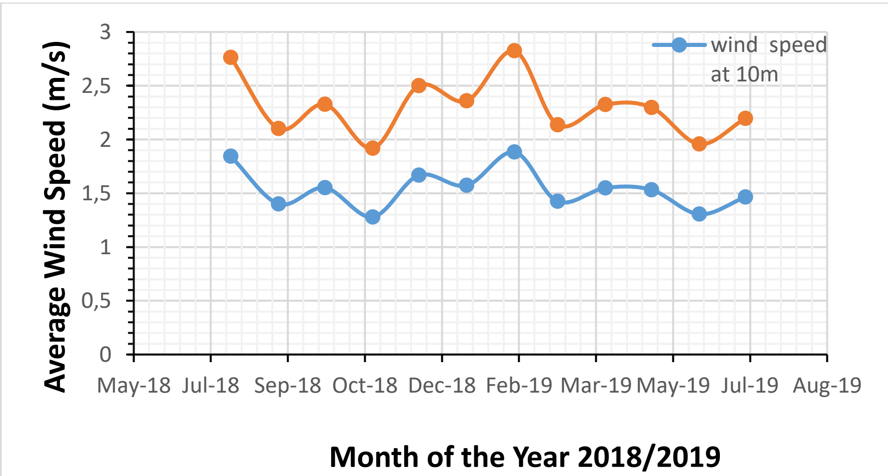

Figure 10: chart of average wind speed upgrade for 2018/2019

Figure 11 shows a more viable wind speed rise in the month between November and March. For this particular year, wind speed is at its high potential in the months between January and February. The chart also shows the rise in wind speed as a result of an increase in hub height, and the significant change in wind speed.

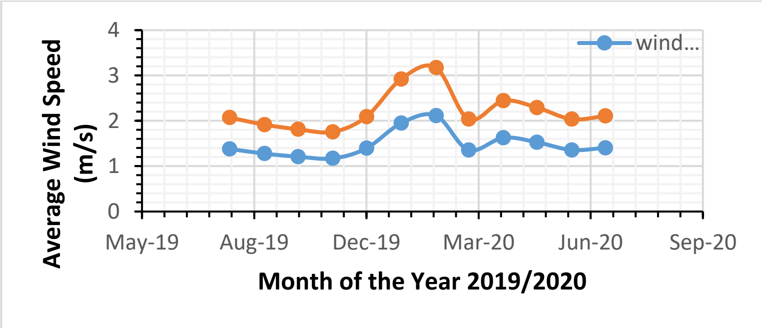

Figure 11: chart of average wind speed at different heights in 2019/2020

The wind speed upgrade for August to December 2020 is also represented in a chart in Figure 12 below. The curve shows the difference in the change in wind upgrade of the year, which is higher in August and September than the rest of the month.

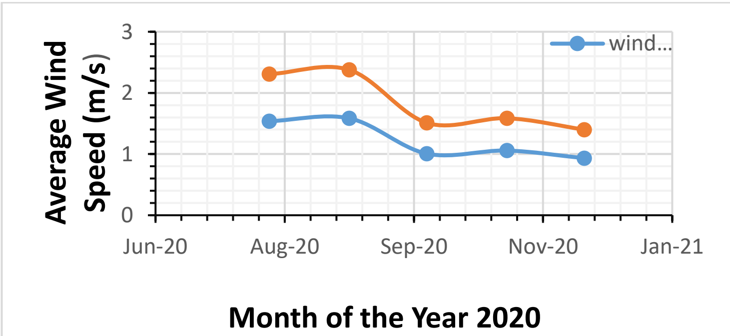

Figure 12: chart of average wind speed upgrade for August to December 2020

The wind upgrade made above the hub height of 50 meters is selected for analysis to determine the electrical power output that can be generated from the wind speed at that hub height. The results obtained are compared with the results obtained from the simulation

Calculating the Power in the Wind

Considering the raw data from NIMET we have a reliable wind speed range of 1.3 m/s to 9.37 m/s at most times of the year, this range is reliable for generating power. Using equation (1) the power in the wind is calculated as;

$\varrho = 1.21\ kg/m^3$; $r = 0.6m$; $A = 1.13112m^2$.

Table 1: The Analysis of The Power in The Wind.

Wind speed at 10 m hub height (m/s)	**Power (w)**
1.3	1.5
9.37	563
Wind speed at 50 m hub height (m/s)	
1.6	2.8
11.93	1,161

The upgraded wind speed and the potential power available in the wind as calculated above in Table 1 fit the operational wind speed of the turbine selected for viable output power.

Table 2 shows a detail of a 1000W wind turbine generator. The power calculated from the wind data acquired for this research is compared with the manufacturer's wind turbine characteristics to see how much power it can generate from the wind energy. The wind turbine parameters are shown in the table below

Table 2: 1kw Qingdao Green New Energy Equipment Co. Ltd Wind Turbine

Model	**S3-1000-B8**	**Blade Material**	**8 pcs**
Rated Power	1000 W	**Rated Voltage**	12v/24v/48v
Wheel Diameter	1.2 m	**Rated Wind Speed**	13 m/s
Cut-in Wind Speed	1.3 m/s	**Survival Wind Speed**	50 m/s
Blade Length	0.58 m	**Height of Tower**	50 m

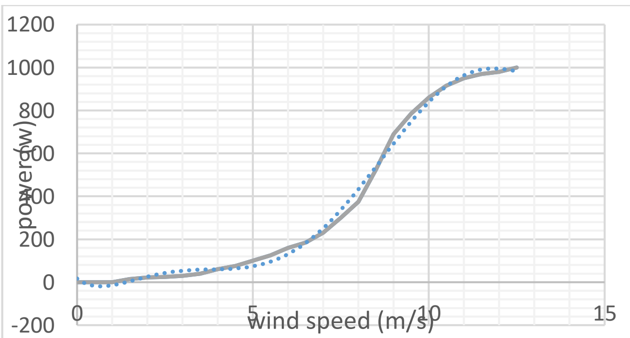

Figure 13: The S3-1000-B8 wind turbine curve

The wind turbine curve in Figure 13 is used to derive the power equation of the turbine by curve fitting using polynomial regression.

Table 3: Seasonal Energy Generated from the wind by the S3-1000-B8 Turbine

DRY SEASON		**RAINING SEASON**		**DRY SEASON**		**RAINING SEASON**	
DATE	**ENERGY (kWh)**	DATE	**ENERGY (kWh)**	DATE	**ENERGY (kWh)**	DATE	**ENERGY (kWh)**
10/2018	**22.464**	04/2019	**17.979**	10/2019	**13.728**	04/2020	**20.597**
11/2018	**14.982**	05/2019	**17.701**	11/2019	**11.225**	05/2020	**16.018**
12/2018	**22.799**	06/2019	**12.812**	12/2019	**16.459**	06/2020	**13.374**
01/2019	**17.139**	07/2019	**15.785**	01/2020	**28.228**	07/2020	**15.510**
02/2019	**20.091**	08/2019	**15.164**	02/2020	**29.949**	08/2020	**18.969**
03/2019	**18.474**	09/2019	**13.837**	03/2020	**15.627**	09/2020	**20316**
TOTAL	**115.949**	TOTAL	**93.278**	TOTAL	**115.216**	TOTAL	**104.784**

In Table 3 we have the seasonal power representation which gives us the amount of power this turbine is generating seasonally

Reservoir Storage Capacity

The total potential energy capacity of a reservoir is given in Equation 4.

$$E(kwh) = \frac{\rho\ (kgm^{-3})\ x\ V\ (m^3)\ x\ g\ (ms^{-2})\ x\ H\ (m)}{3.6\ x\ 10^6\ J(kwh)^{-1}} \qquad \ldots 4$$

Where ρ is the air density, V is the wind speed, g is the acceleration due to gravity, H is the reservoir height and E is the potential energy of the stored water in the reservoir.

We can use this equation to calculate the volume of water pumped for every kWh of power generated. Simplifying equation (5) we have;

$$V(m^3) = E(kwh)\ x\ 14.679 \qquad \ldots 5$$

The curve in Figure 14 below shows the volume of the water pump for every kWh of power using equation (5).

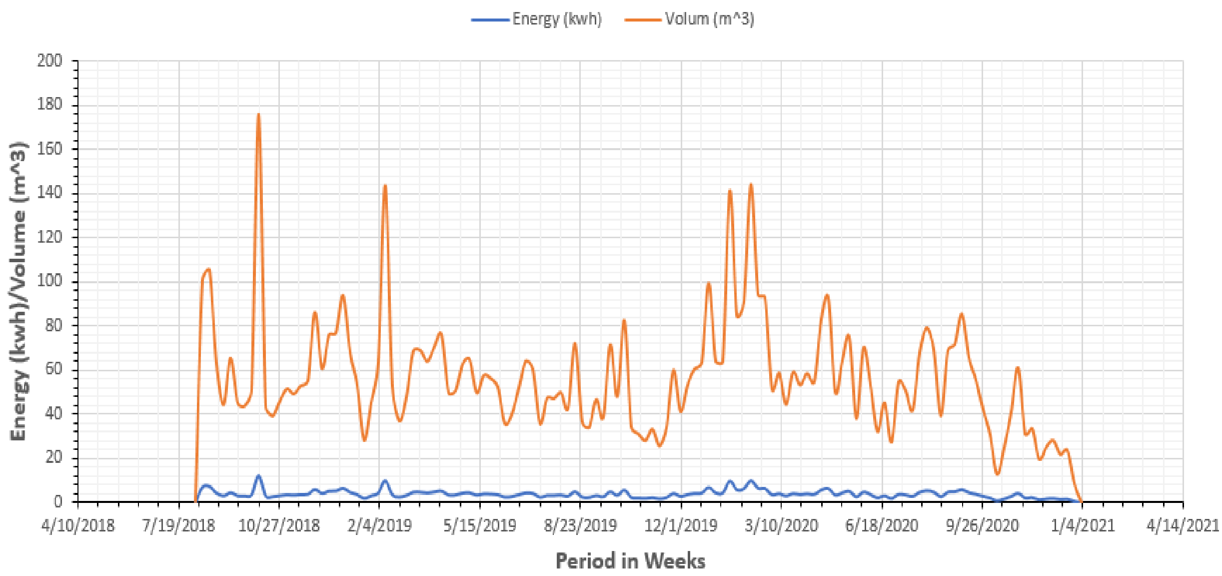

Figure 14: Weekly Energy and Volume of Water Curve

From the table, the minimum volume of water supply to the reservoir from the sum of energy generated weekly by a single S3-1000-B8 wind turbine is 8.765 m^3 and 176 m^3 at its maximum weekly sum of energy generated.

The volume of water required for irrigation per day is 60 m^3 to irrigate a farmland size of 10,000 m^2 and 180 m^3 for a week and 720 m^3 for an autonomous period of a month if no sufficient energy is generated for a month. Considering the minimum volume of water pumped in a week, the minimum number of turbines required to pump irrigation water for a week is;

$$\text{Number of turbines required} = \frac{180m^3}{8.765m^3} = 20.5 \quad ...6$$

Therefore, a minimum of 21 wind turbines (S3-1000-B8) is required for wind farms.

Wind speed and wind power analysis of a wind turbine for Farm irrigation.

The purpose of this analysis is to study and analyze the nature of the wind speed distribution recorded at the Jos plateau and determine the feasibility of the physical implementation of a wind turbine capable of raising water to a tank over a height and using it for both irrigation and power accessories.

The selected parameters used for this simulation are given in Table 4 and Table 5 as follows:

Table 4: Turbine physical parameters

No.	Parameter	Value
1.	Turbine reference height	10 m
2.	Turbine reference altitude	50 m
3.	Surface wind speed	3 m/s
4.	Turbine radius	2.8 m
5.	Turbine efficiency	0.7

Table 5: Related parameters

No.	Parameter	Value
1.	Selected months	24
2.	Air density	1.225 kg/m^3
3.	Stability parameter	0.14
4.	Power coefficient	0.45

The raw wind speed data analysis and power generated.

Figure. 15 is the time distribution of a raw wind speed recorded over 2 years between January 2019 to December 2020. The data were recorded at 15-minute intervals resulting in 96 total daily collected samples, 2880 total monthly recorded samples, and a total of 69,120 wind recorded samples.

The 2-year wind speed data is extracted from a previously recorded 3-year full data (over 88,000 samples). The **MATLAB** command [**WindDat**a = **xlsread** (**'PLATEAU.xlsx', 'C2:C83838'**)] is used to read the raw data. The time waveform shows the very stochastic nature of the wind energy. Figure. 15(**a**) is raw wind data that has not been processed and the histogram of the wind speed distribution in Figure. 15(**b**) shows that the wind speed is biased and not distributed uniformly throughout the period under consideration while the energy derivable from the wind speed is shown in Figure.15(**c**). The **subsequent sections** are determined to present averages of the wind speed distribution to enable ease of analysis and clear visualization of the kind of wind power that can be derived in every segment period. Thus, the data spit over: I. Hourly averaged, II. Daily averaged and III. Monthly averaged wind speed time waveforms, histograms, and wind power.

The monthly averaged wind speed data analysis and power generated.

Figure. 16(**a**) is the wind speed samples averaged over a month while Figure. 16(b) shows the distribution histogram and from the histogram, it could be inferred that the energy generation is better by monthly averaging because the mean is moving much closer to the center of the wind speed distribution. Figure. 16 shows the cumulative sum of wind energy on a logarithmic scale.

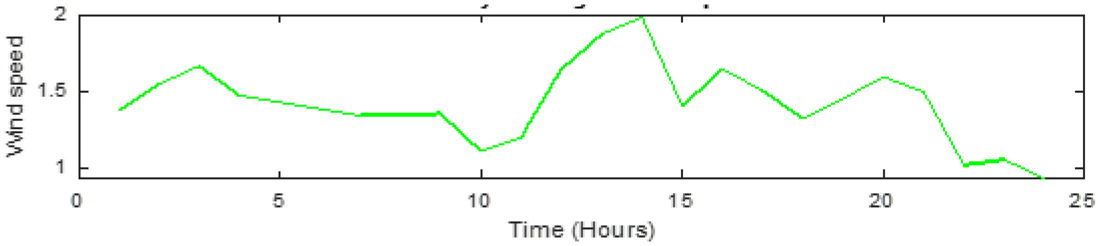

Figure 16(a): Monthly Average Wind Speed waveform

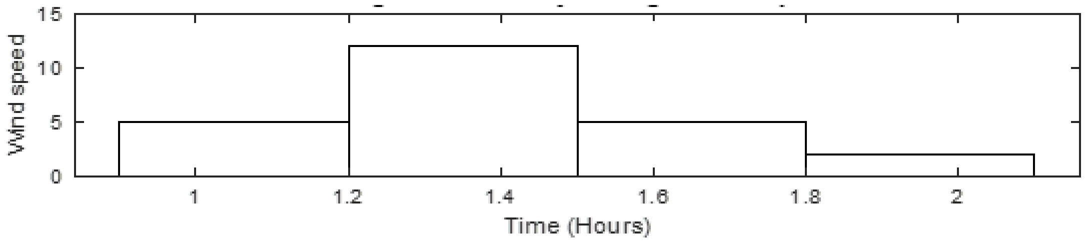

Figure 16(b): Monthly Average Wind Speed Histogram

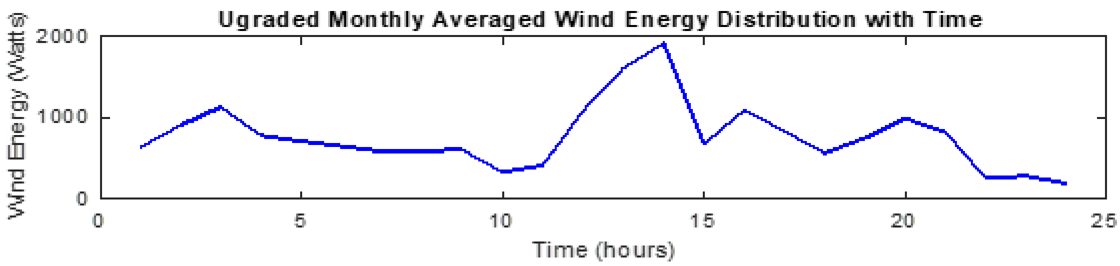

Figure 16(c): Monthly Average Wind Energy

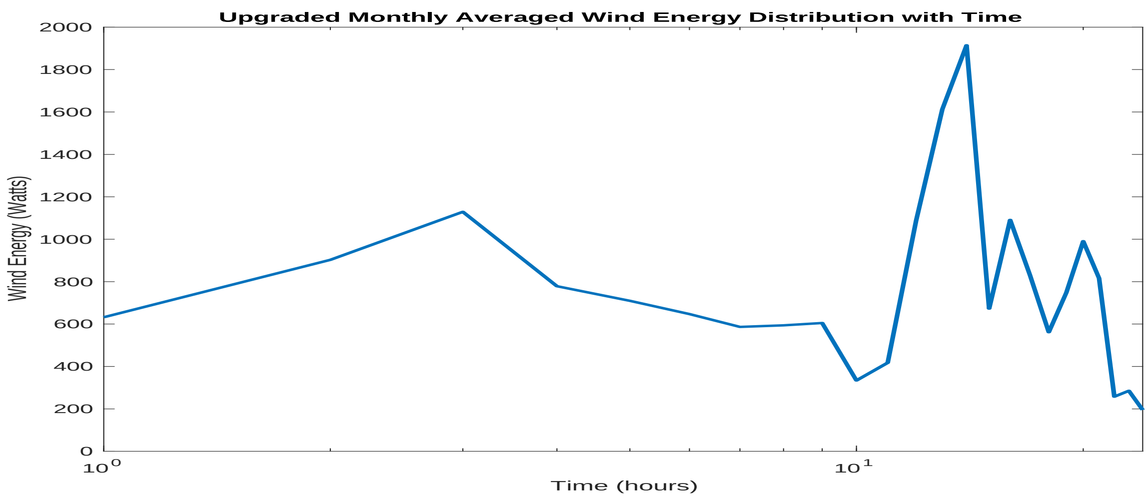

Figure 16: Monthly Average Wind Energy generated

Seasonal wind speed data analysis and power generated.

Figure. 17 is the wind speed measurement considered based on the seasonal period. In Figure. 17(**a**), 17(**b**), and 17(**c**), the wind speed data are recorded based on the seasons within the 2 years between January 2019 and December 2020 (24 months). The periods of the recorded wind speed data are broken on a 6-month basis in Table 6:

Table 6: Seasons from Raw Wind Data

Season/Range of period	Label	Time length	No. of samples
April 2019 to Sept 2019	Season 1	6 months	17280
Oct. 2019 to March 2020	Season 2	6 months	17280
April 2020 to Sept 2020	Season 3	6 months	17280
Oct. 2020 to March 2021	Season 4	6 months	17280
TOTAL			69120

Hourly averaged seasonal Upgraded wind speed data analysis and power generated.

Figure 17 shows the seasonal wind speed distribution while samples Figure. 17 are the corresponding generated wind power over the 3 seasons.

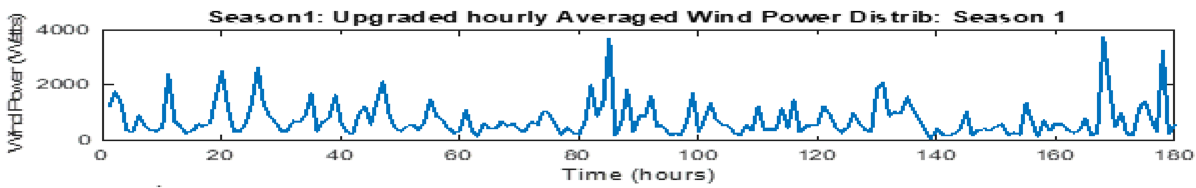

Figure 17(a): Season 1 Upgraded Wind Power Distribution

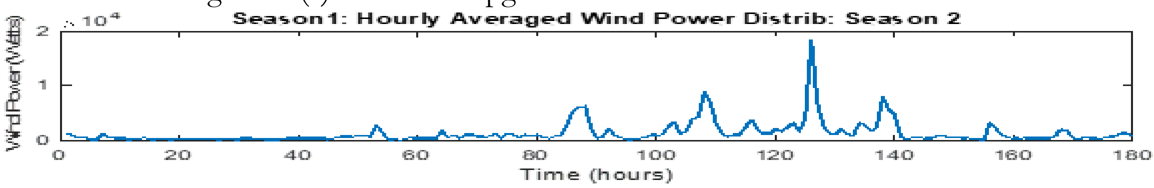

Figure 17(b): Season 2 Upgraded Wind Power Distribution

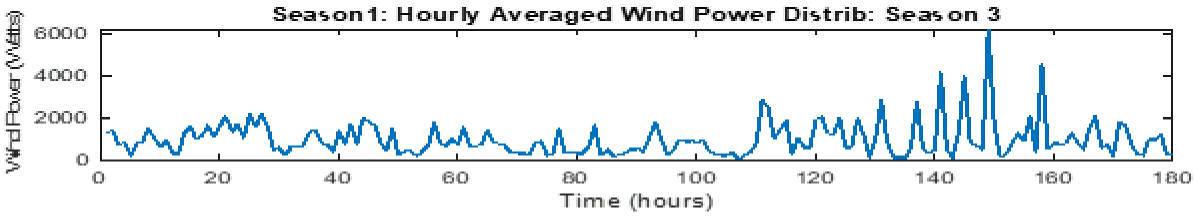

Figure 17 (c): Season 3 Upgraded Wind Power Distribution
Figure 17: Upgraded Averaged Wind Power

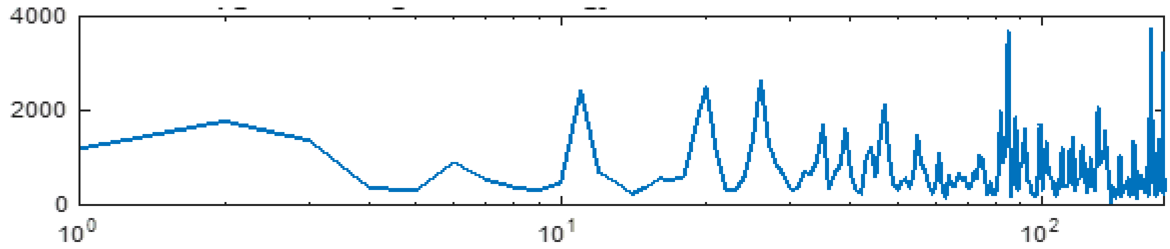

Figure 18(a): Season 1 Upgraded Average Wind Energy Distribution with Time

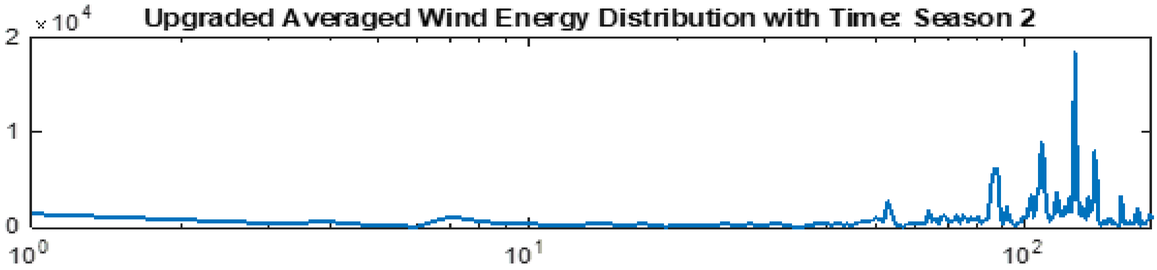

Figure 18(b): Season 2 Upgraded Average Wind Energy Distribution with Time

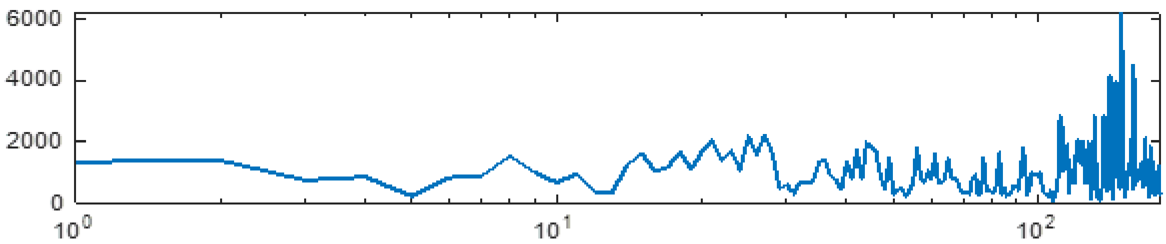

Figure 18(c): Season 3 Upgraded Average Wind Energy Distribution with Time

Figure 18: Upgraded averaged wind power (logarithmic scale) (W)

Raising the water to the upper reservoir

Raising the water requires the energy generated by the wind turbine to be expelled as work done against gravity in the presence of raising the water to a predetermined height. Selected parameters are chosen to model the process as shown in Table 7.

Table 7: Related parameters

No.	Parameter	Value
1.	Gravity	9.8 m/s^2
2.	Upper reservoir height	25 m
3.	reservoir volume	720 m^3
4.	Turbine efficiency	0.7

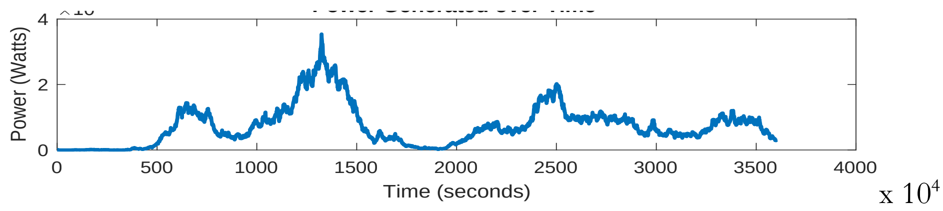

Figure. 19(a): Power Generated Over the Period of 0ne Year

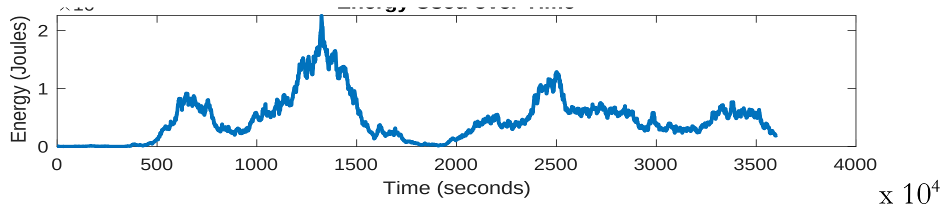

Figure. 19(b): Energy Used over One Year

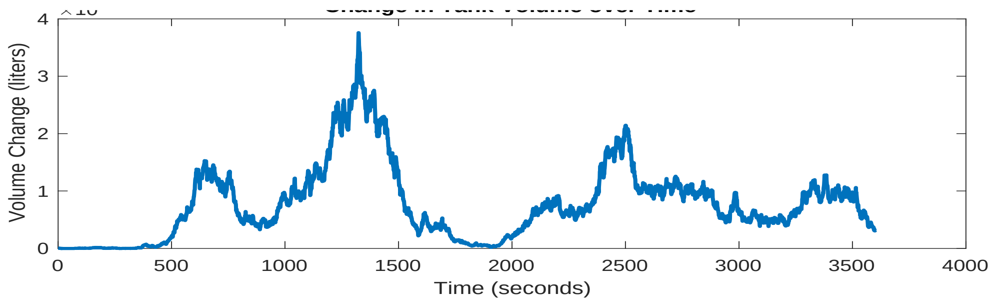

Figure 20(a): Change in Reservoir Volume over One Year

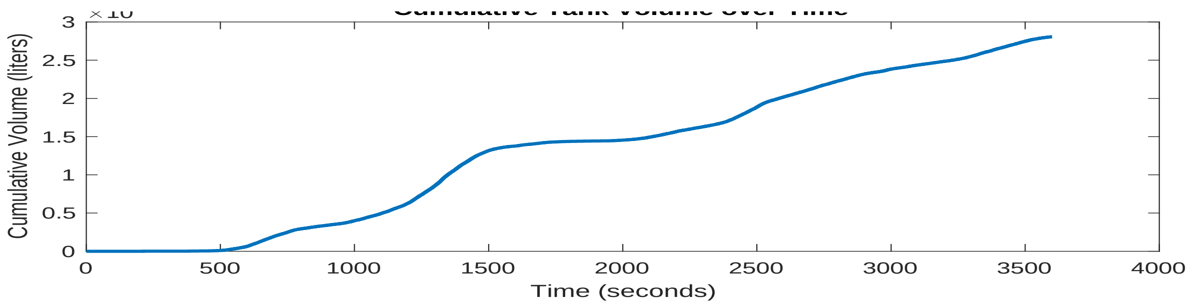

Figure 20(b): cumulative reservoir volume over One Year

CONCLUSION

The overall aim of this work is the feasibility study of an automatic irrigation scheme on the Jos Plateau using wind power to minimize fuel and labor costs. The nature of the terrain at the experimental location will allow the installation of a pump storage hydro system due to the difference in height between the lower and upper reservoirs.

The single wind turbine can generate an average energy of 16kWh in a month and the wind farm of 21 turbine generators can generate a combined average energy of 336kWh with the potential to pump water to the upper reservoir for storage.

The system can collect soil moisture data from the farm, monitor and control irrigation operations. The comparative cost analysis shows that the wind power irrigation system is cheaper with very low maintenance and with a return investment of about 4 years.

REFERENCES

Adenugba, F., & Misra, S. (2019). *Smart irrigation system for environmental sustainability in Africa : An Internet of Everything (IoE) approach*. *16*(December 2018), 5490–5503. https://doi.org/10.3934/mbe.2019273

Akour, S. N., Al-Heymari, M., Ahmed, T., & Khalil, K. A. (2018). Experimental and theoretical investigation of micro wind turbine for low wind speed regions. *Renewable Energy*, *116*, 215–223. https://doi.org/10.1016/j.renene.2017.09.076

Azad, A. K., Rasul, M. G., Islam, R., & Shishir, I. R. (2015). Analysis of wind energy prospect for power generation by three Weibull distribution methods. *Energy Procedia*, *75*, 722–727. https://doi.org/10.1016/j.egypro.2015.07.499

Duker, A., Cambaza, C., Saveca, P., Ponguane, S., Mawoyo, T. A., Hulshof, M., Nkomo, L., Hussey, S., Van den Pol, B., Vuik, R., Stigter, T., & van der Zaag, P. (2020). Using nature-based water storage for smallholder irrigated agriculture in African drylands: Lessons from frugal innovation pilots in Mozambique and Zimbabwe. *Environmental Science and Policy*, *107*(December 2019), 1–6. https://doi.org/10.1016/j.envsci.2020.02.010

Hyams, M. A. (2012). Wind energy in the built environment. *Metropolitan Sustainability: Understanding and Improving the Urban Environment*, 457–499. https://doi.org/10.1533/9780857096463.3.457

Javed, M. S., Ma, T., Jurasz, J., & Amin, M. Y. (2019). Solar-wind-pumped hydro energy storage systems: review and future perspective. *Renewable Energy*. https://doi.org/10.1016/j.renene.2019.11.157

Mentis, D., Hermann, S., Howells, M., Welsch, M., & Siyal, S. H. (2015). Assessing the technical wind energy potential in Africa a GIS-based approach. *Renewable Energy*, *83*, 110–125. https://doi.org/10.1016/j.renene.2015.03.072

Ohunakin, O. S. (2011). Assessment of wind energy resources for electricity generation using WECS in. *Renewable and Sustainable Energy Reviews*, *15*(4), 1968–1976. https://doi.org/10.1016/j.rser.2011.01.001

Ohunakin, O. S., Adaramola, M. S., & Oyewola, O. M. (2011). Wind energy evaluation for electricity generation using WECS in seven selected locations in Nigeria. *Applied Energy*, *88*(9), 3197–3206. https://doi.org/10.1016/j.apenergy.2011.03.022

Ohunakin, O. S., & Akinnawonu, O. O. (2012). Assessment of wind energy potential and the economics of wind power generation in Jos, Plateau State, Nigeria. *Energy for*

Sustainable Development, *16*(1), 78–83. https://doi.org/10.1016/j.esd.2011.10.004

Olayide, O. E., Tetteh, I. K., & Popoola, L. (2016). Differential impacts of rainfall and irrigation on agricultural production in Nigeria: Any lessons for climate-smart agriculture? *Agricultural Water Management*, *178*, 30–36. https://doi.org/10.1016/j.agwat.2016.08.034

Oyaniran, T. (2020). Current State of Nigeria Agriculture and Agribusiness Sector. *AfCFTA Workshop*, *September*, 1–14. https://www.pwc.com/ng/en/assets/pdf/afcfta-agribusiness-current-state-nigeria-agriculture-sector.pdf

Saras, I., Mart, G., Platero, C. A., & S, Á. (2018). *Dual Frequency Regulation in Pumping Mode in a Wind – Hydro Isolated System*. https://doi.org/10.3390/en11112865

Usman, H. M., Mahmud, M., Yahaya, M. S., & Saminu, S. (2024). Wind-Powered Agriculture: Enhancing Crop Production and Economic Prosperity in Arid Regions. *Elektrika*, *16*(1), 10. https://doi.org/10.26623/elektrika.v16i1.8999